IBRACON Structures and Materials Journal
Revista IBRACON de Estruturas e Materiais
ISSN 1983-4195 ismj.org

ORIGINAL ARTICLE

Multi-objective optimization for bridge and viaduct design: case study

Otimização multiobjetivo de projeto de pontes e viadutos: estudo de caso

Eduardo Vicente Wolf Trentini[a]
Guilherme Aris Parsekian[b]
Túlio Nogueira Bittencourt[c]

[a]Universidade Federal de Uberlândia – UFU, Faculdade de Engenharia Civil, Uberlândia, MG, Brasil
[b]Universidade Federal de São Carlos – UFSCar, Programa de Pós-graduação em Engenharia Civil, São Carlos, SP, Brasil
[c]Universidade de São Paulo – USP, Escola Politécnica, São Paulo, SP, Brasil

Received 27 May 2024
Revised 19 July 2024
Accepted 30 August 2024

Abstract: This article presents the application of the Multiple Objective Particle Swarm Optimization (MOPSO) method, enhanced with specifically tuned parameters using the Taguchi method, for optimizing bridge and viaduct designs. Unlike conventional approaches, the optimization in this study encompasses the entire structure rather than focusing solely on the deck. This approach is illustrated through case studies on two viaducts located in Atalaia and Mandaguaçu along the BR-376 highway in Paraná, Brazil. In Atalaia, the optimized solutions achieved reductions in construction costs by 10.5% to 22.7%, CO_2 emissions by 8.9% to 21.2%, and extended the design service life by 24.0% to 540.7%. Similarly, in Mandaguaçu, the optimizations resulted in cost reductions ranging from 9.1% to 23.2%, decreases in CO_2 emissions from 12.7% to 23.5%, and increases in the design service life by up to 540.7%. The study also revealed consistent patterns between the degrees of freedom and objective functions; specifically, larger cross-sectional dimensions tended to lower costs, while smaller dimensions were associated with reduced CO_2 emissions. These findings illustrate the real-world performance improvements afforded by the optimization process, which not only reduces the global cost per year of service compared to the original designs but also enhances economic and environmental performance, thereby demonstrating the effectiveness of MOPSO in structural optimization for sustainable infrastructure development.

Keywords: bridge, viaduct, multiple objective particle swarm optimization, structural optimization, sustainable infrastructure development.

Resumo: Este artigo apresenta a aplicação do método de Otimização por Enxame de Partículas com Múltiplos Objetivos (*Multiple Objective Particle Swarm Optimization*, MOPSO), aprimorado com parâmetros especificamente ajustados pelo método de Taguchi, para a otimização de projetos de pontes e viadutos. Diferente das abordagens convencionais, a otimização neste estudo engloba toda a estrutura, em vez de se concentrar apenas no tabuleiro. Essa abordagem é ilustrada por meio de estudos de caso em dois viadutos localizados em Atalaia e Mandaguaçu ao longo da rodovia BR-376 no Paraná, Brasil. Em Atalaia, as soluções otimizadas alcançaram reduções nos custos de construção de 10,5% a 22,7%, emissões de CO_2 de 8,9% a 21,2%, e estenderam a vida útil do projeto de 24,0% a 540,7%. De forma similar, em Mandaguaçu, as otimizações resultaram em reduções de custo de 9,1% a 23,2%, diminuição das emissões de CO_2 de 12,7% a 23,5%, e aumentos na vida útil do projeto de até 540,7%. O estudo também revelou padrões consistentes entre os graus de liberdade e as funções objetivas; especificamente, dimensões transversais maiores tendiam a reduzir custos, enquanto dimensões menores estavam associadas a reduções nas emissões de CO_2. Esses achados ilustram as melhorias de desempenho no mundo real proporcionadas pelo processo de otimização, que não apenas reduz o custo global por ano de serviço em comparação com os projetos originais, mas também aprimora o desempenho econômico e ambiental, demonstrando assim a eficácia do MOPSO na otimização estrutural para o desenvolvimento de infraestruturas mais sustentáveis.

Palavras-chave: ponte, viaduto, otimização por enxame de partículas com múltiplos objetivos, otimização estrutural, desenvolvimento de infraestrutura sustentável.

Corresponding author: Eduardo Vicente Wolf Trentini. E-mail: etrentini@ufu.br
Financial support: This study was financed in part by the Coordenação de Aperfeiçoamento de Pessoal de Nível Superior – Brasil (CAPES) – Finance Code 001.
Conflict of interest: Nothing to declare.
Data Availability: The results presented in this article can be replicated using the compiled software or algorithms described in this article. All necessary data and source code are made openly accessible to reproduce the results. The resources can be found at our GitHub repository https://github.com/evwtrentini/optimusviaduto and the project's dedicated website https://www.optimusviaduto.ufscar.br.

How to cite: E. V. W. Trentini, G. A. Parsekian, and T. N. Bittencourt, "Multi-objective optimization for bridge and viaduct design: case study," *Rev. IBRACON Estrut. Mater.*, vol. 18, no. 1, e18104, 2025, https://doi.org/10.1590/S1983-41952025000800004

1. INTRODUCTION

The design of bridges and viaducts typically begins with a preliminary assessment, when engineers use their expertise to outline key structural features. This includes determining the dimensions and layout of elements such as columns and specifying the concrete's strength. Following this initial phase, the process moves on to the structural analysis and limit state design. With the broad range of possible configurations, multiple alternative designs can aid in choosing the best-performance solution requirements, considering aspects such as lower cost, shorter construction timelines, reduced environmental impacts, and longer service lives.

The optimization process focuses on selecting an optimal set of parameters, known as Degrees of Freedom (DOF), to either maximize or minimize a defined objective function. These parameters define the characteristics of the structural solution, such as dimensions and material properties. Increasing the DOF within this process facilitates a more thorough exploration of potential solutions, thereby enhancing the overall outcomes.

In the realm of multi-objective optimization, where different objectives may conflict with one another, it is misleading to label any solution as absolutely "optimal". As Hashimoto [1] notes, a solution may favor one objective at the expense of others, leading to inevitable trade-offs. The output of an optimization process is a set of compromise solutions, each evaluated and ranked based on the principle of Pareto dominance.

The field of structural cost optimization is extensive, yet research specifically targeting bridges and viaducts is relatively scarce. The literature reviews by Hassasain and Loov [2] and Trentini [3] present a total of twenty-three studies.

The foundational study by Torres et al. [4] introduced the use of linear programming to derive cost-optimal designs for single-span, prestressed, and precast bridges. They incorporated AASHO beams in their software database, concluding that optimal girder spacing is roughly 2.75 meters and lighter vehicle types can broaden the range of viable design solutions. Lounis and Cohn [5] applied a nonlinear optimization method using the GAMS/MINOS software, concluding that simply supported decks are cost-efficient up to 27 meters, while spans of 28 to 44 meters and 55 to 100 meters are best served by two and three continuous spans, respectively.

Olivieri [6] developed a genetic algorithm in Visual Basic to optimize the costs of prestressed concrete bridge decks, which included I-section, precast, prestressed, and simply supported girders. His analysis yielded cost savings ranging from 2.57% to 13.13%. Cortês [7] employed a genetic algorithm to optimize the same type of bridge decks, yielding significant cost reductions ranging from 13.6% to 26.8%. Ahsan et al. [8] expanded the scope by using an evolutionary optimization algorithm for I-section girder bridge decks and by increasing the number of degrees of freedom in the optimization process, yielding a substantial cost reduction of 35.4%. It should be noted that the extent of cost reduction depends on the quality of the solution used as a reference.

Building on the exhaustive search approach, Trentini [3] developed an optimization method implemented using MATLAB to optimize the cross-sections of bridge decks featuring multiple precast and post-tensioned I-section girders. El Mourabit [9] extended the optimization to encompass the entire bridge structure, specifically focusing on single-beam bridge decks, and achieved a 12.8% cost reduction. This methodology did not include the costs associated with the foundations, which could potentially alter the reported cost savings. Yepes et al. [10] applied multi-objective optimization specifically to the bridge decks of I-section beams, achieving a 233% improvement in service life and an 11% reduction in CO_2 emissions, with only a 4% increase in optimal cost.

García-Segura et al. [11] conducted a multi-objective optimization study on cellular bridge decks, focusing on cost, CO_2 emissions, and safety factors. They used a harmony search algorithm and an artificial neural network trained with CSiBridge data to efficiently estimate structural analysis results, balancing precision with computational speed.

Table 1 provides a summary of key studies in the field of structural optimization for bridge structures. This overview highlights the structure types, the number of degrees of freedom (DOF) considered in each study, the optimization methods employed, the specific objectives targeted, and the key results obtained from each research.

The progression of research in deck optimization has seen a consistent increase in the number of DOFs, from the early studies by Torres et al. [4] to the more comprehensive approaches by Ahsan et al. [8]. This has led to a progressively finer refinement of the optimal solution. El Mourabit [9] extended the scope of optimization beyond the deck to encompass the entire bridge structure, including the position of the columns. García-Segura et al. [11] identified a correlation between the initiation of corrosion and construction costs, a dynamic yet to be investigated in the context of precast post-tensioned I-girder bridges and viaducts.

Table 1. Summary of studies

Researcher(s)	Structure Type	DOF	Optimization Method	Objective function	Key Results
Torres et al. [4]	Precast I-girders bridge deck	2	Linear Programming	Cost	Optimal girder spacing of 2.75 meters
Lounis and Cohn [5]	Bridge with precast post-tensioned I-girders deck	4	Nonlinear Optimization	Cost	Cost-effective decks for spans up to 100 meters
Olivieri [6]	Precast prestressed I-girders bridge deck	4	Genetic Algorithm	Cost	Cost reductions between 2.57% and 13.13%
Cortês [7]	Precast prestressed I-girders bridge deck	7	Genetic Algorithm	Cost	Cost reductions from 13.6% to 26.8%
Ahsan et al. [8]	Precast post-tensioned I-girders bridge deck	11	Evolutionary Optimization Algorithm	Cost	35.4% cost reduction
Trentini [3]	Precast post-tensioned I-girders bridge deck	5	Exhaustive Search	Cost	16.42% cost reduction
El Mourabit [9]	Reinforced concrete beam bridge	9	Genetic Algorithm and Pattern Search	Cost	12.8% cost reduction
Yepes et al. [10]	Reinforced concrete I-beam	20	Simulated Annealing	Cost, CO_2 emission, Service life	Service life increased by 233%, CO_2 reduction by 11%, with a 4% increase in optimal cost
García-Segura et al. [11]	Post-tensioned concrete box-girder bridge deck	34	Multi-objective harmony search	Cost, CO_2 emission, Safety factor	With a small cost increment, the safety and durability can be significantly improved

This research focuses on metaheuristic methods for solving multi-objective optimization problems. According to Blum and Roli [12], these methods use high-level strategies to guide heuristics in the search for near-optimal solutions. Zavala et al. [13] found that NSGA-II, SPEA2, and MOPSO were the most commonly studied algorithms, with 20, 7, and 5 papers, respectively.

The No-Free-Lunch theorem, proposed by Wolpert and Macready [14], states that no single optimization method is superior for all problems, meaning algorithms must be tested and calibrated for each specific case.

Recently, Trentini et al. [15] developed a methodology for the optimization of bridges and viaducts composed of post-tensioned, precast I-girders, rectangular crossbeams, circular columns, and deep caisson foundations, integrating criteria of structural efficiency and sustainability. The research focuses on optimizing cost, environmental impact and service life in structural design. The proposed methodology generates a set of multi-objective compromise solutions, identifying the optimal geometry, concrete type, and level of post-tensioning. Various metaheuristic algorithms were evaluated, including Multiple Objective Particle Swarm Optimization (MOPSO), Nondominated Sorting Genetic Algorithm II (NSGA-2), and Strength Pareto Evolutionary Algorithm 2 (SPEA2), with MOPSO proving to be the most effective for this problem. Calibration of parameters plays an important role in optimization techniques, as the settings of these parameters markedly affect the method's performance and efficacy. The MOPSO parameters were calibrated, for this specific problem, using the Taguchi method, increasing the average hypervolume.

The objective of this research is to assess the effectiveness of MOPSO, calibrated by Trentini et al. [15], for optimizing bridge and viaduct designs in real-world settings and to explore the trade-off relationships among objective functions at the Pareto optimal front. Additionally, the study aims to identify patterns in the relationships between the degrees of freedom of optimal solutions across different areas of this front. To achieve these goals, the methodology will be applied in two case studies involving actual viaducts constructed on the BR-376 highway in Paraná, Brazil. The first case study focuses on a viaduct at the entrance of Atalaia city, and the second in Mandaguaçu city. The paper is

organized as follows: Section 2 outlines the optimization problem that will be addressed; Section 3 details the methodology applied to solve this optimization problem; Section 4 presents the case studies and discusses the findings; finally, Section 5 provides a summary of the results and outlines their conclusions.

2. OPTIMIZATION: PROBLEM DESCRIPTION

As this study aims to optimize multiple objectives simultaneously, it falls under the category of multi-objective optimization problems. Such problems are formally defined as follows:

minimize the Equation 1

$$\boldsymbol{y} = \boldsymbol{F}(\boldsymbol{x}) = [f_1(\boldsymbol{x}), f_2(\boldsymbol{x}), \dots, f_m(\boldsymbol{x})] \tag{1}$$

subject to the constraint of Equation 2 and Equation 3

$$g_j(\boldsymbol{x}) \leq 0, j = 1,2, \dots, p \tag{2}$$

$$h_k(\boldsymbol{x}) = 0, k = 1,2, \dots, q \tag{3}$$

where:

$\boldsymbol{y} = (f_1, f_2, \dots, f_m) \in Y$: denotes the objectives vector with dimension m and Y is the objective space ;

$f_i(\boldsymbol{x})(1 = 1,2, \dots, m)$: denotes the i-th objective function among a total of m functions in the problem.

In this context, the vector $\boldsymbol{x}$ encapsulates the design characteristics of bridges or viaducts, including parameters like the number of girders, slab height, and the characteristic concrete strength of the columns. Detailed descriptions of the decision vector, which has a dimension n based on the number of spans N_v, are provided in section 2.2 and defined by Equation 5. The objectives vector $\boldsymbol{y}$ comprises functions such as construction cost, environmental impact, and design service life, as discussed in section 2.1. Finally, the constraint inequalities g_j and the equality constraints h_k are established according to standards ensuring structural safety and performance, detailed in section 2.3.

2.1. Objective functions

This study examines multi-objective optimization, which optimizes multiple objective functions concurrently. The focus is on optimizing three specific objectives: construction cost, environmental impact via CO_2 emissions, and design service life, which often conflict. For example, enhancing the service life of a structure might require more concrete cover, increasing both costs and CO_2 emissions. On the contrary, cost-reduction efforts might promote using more concrete with less reinforcement, which, while cost-effective, boosts CO_2 emissions. Meanwhile, minimizing CO_2 emissions may involve using less concrete and more reinforcement, potentially raising costs and affecting the service life negatively. This showcases the intricate conflicts within the optimization problem, as efforts to improve one objective could deteriorate others.

The cost function in this study specifically seeks to minimize the total cost, which is calculated by summing the unit costs for all required materials, manufacturing services, and installations, each multiplied by its respective quantity. Unit costs are obtained from the Sistema de Custos Referenciais de Obras (SICRO) [16] and expert firms. Updates to these costs are regularly provided by the Departamento Nacional de Infraestrutura de Transportes (DNIT), which organizes the data by state and date. As specified in DNIT's publication [16], the service compositions used for estimating costs, particularly for São Paulo as of April 2022, are detailed in [15].

The function for CO_2 emissions aims to minimize the total emissions from all construction-related inputs and services, thereby evaluating the environmental impact. This assessment specifically measures the total CO_2 emissions associated with the construction process. To estimate these emissions, this study employs the Carbon Emissions Quantification Method (QE-CO_2 Method) proposed by Costa [17]. This approach accounts for emissions from the extraction of raw materials, their transportation, and the production stages prevalent in the Brazilian construction industry. Total CO_2 emissions are determined by applying the emission factor to each input or service used, as specified in Costa's method. The emission factors employed in this study are defined in [15].

The design service life, which is intended to be maximized, is determined a priori by the time required for depassivation of the reinforcement. This criterion was chosen due to its relatively low computational cost, considering the large number of evaluations of this function during the optimization process. Additionally, more elaborate methods for estimating design service life are unlikely to significantly alter the relative service life outcomes among the solutions being compared during the optimization process. This, in turn, would not materially affect the resulting set of optimal solutions.

The methodology of Possan et al. [18] is used to estimate the carbonation depth at age t, with the design service life defined by the semi-probabilistic method using Monte Carlo simulation; more details about the probability distribution functions used can be found in [15]. The depassivation time of the reinforcement t_d for each simulation is defined by Equation 4, obtained by equating the carbonation depth of the concrete to the cover of the structural element c.

where:

$$t_d = \frac{20 \cdot c^2}{\left(k_c \cdot \left(\frac{20}{f_{ck}}\right)^{k_{fc}} \cdot exp\left[\left(\frac{k_{ad} \cdot ad^{\frac{3}{2}}}{40 + f_{ck}} \right) + \left(\frac{k_{CO_2} \cdot {CO_2}^{\frac{1}{2}}}{60 + f_{ck}} \right) - \left(\frac{k_{UR} \cdot (UR - 0.58)^2}{100 + f_{ck}} \right) \right] \cdot k_{ce} \right)^2} \quad (4)$$

t_d: design service life; c: cover; f_{ck}: characteristic resistance of concrete; k_c: factor referring to the cement type; k_{ce}: factor related to exposure to rain; k_{fc}: factor referring to the resistance of concrete; UR: relative humidity in average; k_{UR}: factor related to relative humidity; CO_2: content of CO_2 in the atmosphere; k_{CO_2}: factor referring to the CO_2 content; ad: content of pozzolanic addition in concrete; and k_{ad}: factor referring to pozzolanic additions. The necessary factors of Equation 4 are detailed in [18].

2.2. Degrees of freedom of the optimization problem

Developing a candidate structural solution entails establishing a set of parameters that characterize the object of study, referred to as the DOF for the optimization problem. These DOFs include parameters related to the positioning of supports, dimensions and material properties of structural elements such as columns, caissons, and girders, among others. The list of these parameters, detailing each specific DOF and their roles in the structural configuration, can be found in [15].

The number of DOFs, n, defining a solution is influenced by the number of spans, N_v. This problem includes eight fixed DOFs that do not depend on the number of spans; examples include reinforcement covers and the characteristic strengths of concrete. Additionally, the problem incorporates variable number of DOF that are dependent on the number of spans in different ways: one DOF is influenced by $N_v - 1$, which relates to the position of each intermediate support. Sixteen DOF directly correspond to the number of spans, such as the height of the slab and the dimensions of the girders. Seven DOF are determined by $N_v + 1$, examples of which include the foundation depth at each support and the dimensions of the pier caps. Consequently, the total number of DOFs for the optimization problem is calculated using the Equation 5.

$$n = 14 + 24N_v \quad (5)$$

2.3. Constraints

In Brazil, the guidelines for this type of structure, often referred to as constraints in optimization processes, are delineated by NBR 7187 [19]. According to this standard, the design of bridges and viaducts must meet all ultimate and service limit states as outlined in NBR 6118 [20], covering all potential action combinations during their construction and usage.

2.3.1. Structural Analysis

Structural analysis is conducted in two primary stages, starting with a specific geometric configuration defined by the pre-set degrees of freedom. Initially, the analysis focuses on the deck's transverse load distribution using the Fauchart process, considering variations in the positioning of the NBR 7188 [21] design vehicle. This is followed by applying these results to a three-dimensional beam model representing the entire structure and its foundations, using the Winkler approach [22] to model soil-structure interactions. The AMEBP3D algorithm, designed for

computationally efficient analysis of beam structures, uses the stiffness method to accommodate hinges, deformation constraints, and flexible supports under various loading conditions. Inputs for the algorithm include the analytical model and load cases, producing outputs such as displacement vectors, support reaction vectors, internal force vectors, and force and moment vectors needed to maintain zero displacement under load. This algorithm, which incorporates Barros and Martha's methodology [23] for handling rigid and inextensible members through the direct stiffness method, optimizes the total potential energy minimization problem with detailed aspects handled by separate pre-processing and processing subroutines to reduce redundancy. Further details about AMEBP3D can be found in Trentini [24].

2.3.2. Structural component design

The bridge deck slabs are classified into end slabs (pined-fixed) and center slabs (fixed-fixed) based on their supports. These moments are calculated using Rüsch tables 14 and 27 for end and center slabs, respectively. Coefficients α_0 and α are then used to adjust these moments for continuity, following the method proposed by [25].

The shear forces in the slabs are evaluated using the concept of effective width for point loads. In addition to the ultimate combination forces, the forces from the frequent combination are also determined to verify the fatigue limit state for the slabs. The longitudinal reinforcement of the slabs is designed based on the simplified rectangular stress block model of NBR 6118 [20], ensuring the limit x_{LN}/d is checked. Once the flexural reinforcement is designed, the stress variation under the frequent combination is calculated and, if necessary, iteratively adjusted to comply with the fatigue limit state as specified in section 23.5.5 of NBR 6118 [20].

Regarding the shear force ultimate limit design, the process begins with checking the concrete strut compressive strength limit. If additional reinforcement is necessary, a rebar truss ribbed slab is selected and its spacing is then evaluated such that the resistant shear force equals the shear force demand, $V_{Rd3} = V_{Sd}$.

The deformation service limit verification of the girders is assessed according to the approach proposed by El Debs [26]. Assuming that the girder meets the cracking limit state, the cross-sectional properties are calculated considering the uncracked section. Time-dependent effects are accounted for using multipliers on the elastic deflection as in PCI [27].

The stability of girders is assessed through a two-stage process prior to their permanent placement on the deck. Initially, girders are examined under only their self-weight without rotational restraints. Subsequently, their stability is checked with additional loads and rotational restraints from transverse members during slab casting. According to NBR 7187 [19], lateral stability of precast beams must also be verified, particularly in transient conditions, utilizing a non-linear analytical approach as described by [28] to ensure stability on elastic supports.

Precast elements, such as girders and slabs, are often bonded on-site to form a monolithic connection, defined as composite members under NBR 9062 [29]. Unlike previous studies that modeled the girder-slab assembly as a single-stage cast, this research considers a two-stage casting process to address strain discontinuities at the interface, aligning with [30].

Pier caps, designed to withstand bending and torsion, have their design forces calculated based on the force envelope. Their design follows the principles for bending and torsion as specified in NBR 6118 [20], section 17.5.1.3.

Columns are analyzed under axial and bending loads, considering second-order effects. According to NBR 7187 [19], cantilever columns are treated as isolated elements using methods from NBR 6118 [20] section 15.8.3.

This methodology utilizes columns and caisson shafts with circular cross-sections of varying diameters, necessitating a foundation block for transition. This transition creates tensile stresses counteracted by horizontal stirrup reinforcement, calculated based on [31]. The caisson shafts are designed for flexural compression using the same methods applied to the columns.

It is common practice to assume no lateral resistance along the caisson shaft, with the entire column load transferred to the ground through the caisson base [32]. The base's allowable resistance is determined by multiplying the allowable soil stress by the area of the caisson's bell bottom. The allowable stress can be calculated using an empirical expression correlating soil penetration resistance with soil stress [33].

3. METHODOLOGY

Particle Swarm Optimization (PSO) is a heuristic technique inspired by the behavior of birds flocking together in search of food. Kennedy and Eberhart [34] highlighted its effectiveness in various optimization problems. Coello et al. [35] adapted this method for multi-objective problems, resulting in the MOPSO algorithm.

The MOPSO algorithm works by evaluating a swarm of potential solutions in each iteration, where each solution is represented by a particle. The position of each particle corresponds to a set of parameters, or DOF, defining that solution. The algorithm tracks two key positions: the personal best, which is the best result a particle has achieved, and the global best, which is the top result among all particles. Particle movement is influenced by a velocity vector, which

is updated in each iteration. This velocity is controlled by the inertia factor W and learning factors that dictate how much a particle is drawn towards either its personal best C_1 or the global best C_2.

In the MOPSO algorithm, let $\boldsymbol{x}^i(t)$ represent the position vector of particle p^i at iteration t. The position of p^i is updated by adding the velocity $\boldsymbol{v}^i(t)$ to the current position, i.e.

$$\boldsymbol{x}^i(t) = \boldsymbol{x}^i(t-1) + \boldsymbol{v}^i(t) \tag{6}$$

The velocity vector, which conveys the socially transmitted information among particles in the swarm, is defined by

$$\boldsymbol{v}^i(t) = W \cdot \boldsymbol{v}^i(t-1) + C_1 \cdot r_1 \cdot \left(\boldsymbol{x}^{mp^i} - \boldsymbol{x}^i(t-1)\right) + C_2 \cdot r_2 \cdot \left(\boldsymbol{x}^{mg} - \boldsymbol{x}^i(t-1)\right) \tag{7}$$

where:
$\boldsymbol{x}^{mg}$: global best position of the swarm;
$\boldsymbol{x}^{mp^i}$: personal best position of particle i;
r_1, r_2: random values between 0 and 1.

The algorithm starts by creating a swarm of particles, each assigned a random position, ensuring that all initial positions are feasible solutions. Each particle's performance is then evaluated based on the objective functions, and its initial personal best is set to its starting position. MOPSO maintains an archive of non-dominated solutions, populated with the best solutions from the first swarm. Figure 1 presents the pseudocode for MOPSO.

During each iteration, the best global position from the particles in the archive is identified, starting the update process. This involves recalculating the velocity vector based on Eq. (7), adjusting the position using Eq. (6), and applying the polynomial mutation operator. The parameter η_m regulates the mutation operator's range. If the new position meets all constraints, its performance is evaluated, and the personal best x^{mp^i} is updated. Otherwise, if the position violates constraints or is infeasible, the personal best remains unchanged.

Algorithm 1. MOPSO Pseudocode

```
t ← 1, A ← Empty()
p ← GenerateInitialSwarm()
A ← UpdateArchive(p,A)
while t < tmax do
    xmg ← SelectGlobalBest(A)
    for each i in  p do
       xmg ← SelectGlobalBest(A)
       v(i) ← UpdateVelocity(x, xmp, xmg)
       x(i) ← UpdatePosition(x, v)
       x(i) ← Mutation(x)
       p(i) ← CheckBoundary(x)
       F(i) ← FitnessEvaluation(x)
       xmp(i) ← UpdatePersonalBest(F)
    end for
    A ← UpdateArchive(p,A)
    t ← t + 1
end while
```

Figure 1. pseudocode for MOPSO

The personal best position is updated when the new position dominates the previous one, or if their performances are incomparable, meaning neither dominates the other. In such cases, there is a 50% probability that the personal best will change to the new position. Once all particle movements are completed and their performances have been evaluated, the archive of non-dominated solutions is updated. This cycle continues for a set number of iterations.

When selecting the best particle from the archive, it is important to consider a density measure that reflects the distance of particles within the archive, given that all archived particles are non-dominated. In MOPSO, this density

measure is the crowding distance. The crowding distance α_i of solution i represents the estimated size of the largest cuboid encompassing i without including any other solutions. Further details on the evaluation of crowding distance can be found in the original article proposing it [36]. During the selection of the global best particle from the archive, particles with the highest crowding distance values are chosen to ensure that the swarm moves towards sparser regions of the search space.

MOPSO relies on a set of tunable parameters to optimize performance. Key parameters such as population size, mutation polynomial index η_m, particle inertia W, and the learning factors (C_1 and C_2) must be adjusted to ensure proper convergence. The Taguchi method, a fast experimental optimization technique, is used to fine-tune these parameters, aiming to identify robust solutions even in the presence of noise from stochastic processes.

The parameters of MOPSO will follow those calibrated by Trentini et al. [15], as they are specifically fine-tuned for this type of problem and offer superior performance in hypervolume and pure diversity. The calibration performed by Trentini et al. [15] utilized the Taguchi method to optimize the parameters. The calibrated parameters are presented in Table 2 and will be used in the case studies.

Table 2. Calibrated Parameters for MOPSO

MOPSO Parameters				
W	C_1	C_2	η_m	Swarm size
0.40	0.75	1.00	20	130

4. RESULTS AND DISCUSSION

In this section, two case studies are detailed, applying the previously proposed and calibrated optimization methodology to two actual viaduct designs that have been constructed. The case studies focus on viaducts located on the BR-376 highway in Paraná, Brazil. The first is situated in the City of Atalaia, and the second in the City of Mandaguaçu.

4.1. Case study of the viaduct in Atalaia

The Atalaia case study involves a viaduct that spans 31 meters, divided into two spans, and measures 14 meters in width, with a level road grade as shown in Figure 2. The N_{spt} used in Figure 2 refers to the Standard Penetration Test *N*-value. Additional details necessary for defining the problem are provided in [24].

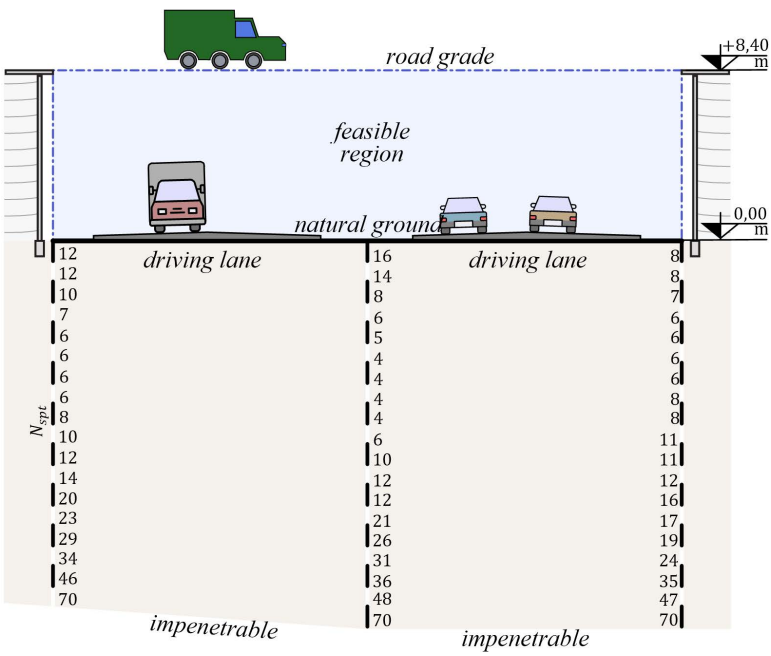

Figure 2. Optimization problem of the first case study – Atalaia

The details of the constructed solution were sourced from the structural design provided by the original engineer of the project. This design incorporates two symmetric spans, each with five girders measuring 1.53 meters in depth and two columns per pier cap, each 100 cm in diameter. The shafts are of the same diameter and reach a depth of 16 meters. Full specifications of this constructed solution are detailed in [24], Figure 3 illustrates this configuration.

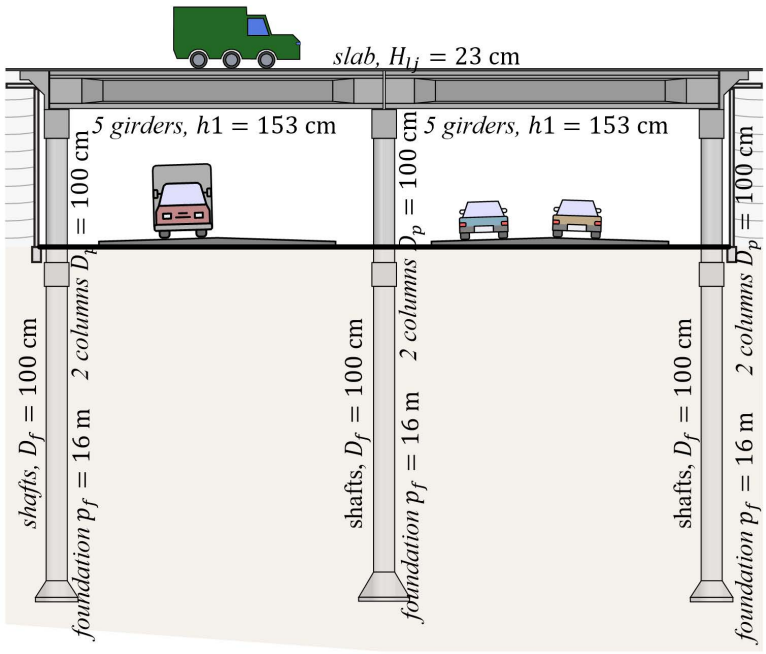

Figure 3. Original configuration of the first case study – Atalaia

For the original design, the values of the objective functions, including construction cost, CO_2 emissions, and design service life, were evaluated as described in section 2.1. The results for these objective functions, based on the design proposed by the project's author, are presented in Table 3.

Table 3. Objective functions for the original solution of the first case study – Atalaia

Construction cost	Environmental impact	Design service life
R$ 1,126,932.29	258.06 tCO_2	51.3 years

The optimization process for this case study was executed on the cluster at the Federal University of São Carlos (Universidade Federal de São Carlos, UFSCar) and completed after 24 hours of analysis. The objective function values of the optimal solutions resulting from this process are depicted in Figure 4.

In the visual representations, such as the objective function values and parallel coordinate plots, each solution is color-coded using a blend of red, green, and blue. Each color corresponds to a specific objective function: red for cost, green for CO_2 emissions, and blue for service life. The intensity of each color increases with the improvement in performance for its corresponding objective: higher intensities of red indicate lower costs, greater intensities of green signal lower CO_2 emissions, and stronger shades of blue denote longer service lives. This method visually communicates the performance of each solution across the various objectives.

When analyzing the solutions, it is observed that the entire optimal set outperforms the original proposal across all objective functions. The optimal solutions achieve a reduction in construction costs ranging from 10.5% to 22.7%, decrease CO_2 emissions by 8.9% to 21.2%, and extend the design service life by 24.0% to 540.7%.

Further analysis of solutions 20, 41, 80, 88, and 122, which all share similar design service lives, reveals a clear relationship between cost and CO2 emissions, as illustrated in Figure 5. For instance, when comparing the objective functions of solution 88 with solution 41, it is possible to reduce environmental impact by 4.8% for an additional cost of only 1.0%. However, this relationship is not consistently proportional; for example, comparing solution 20 with

solution 122 results in a 4.3% cost reduction but only a 0.5% increase in CO_2 emissions. These solutions have an average project lifespan of 251 years, but these proportions hold true for any range of design service life.

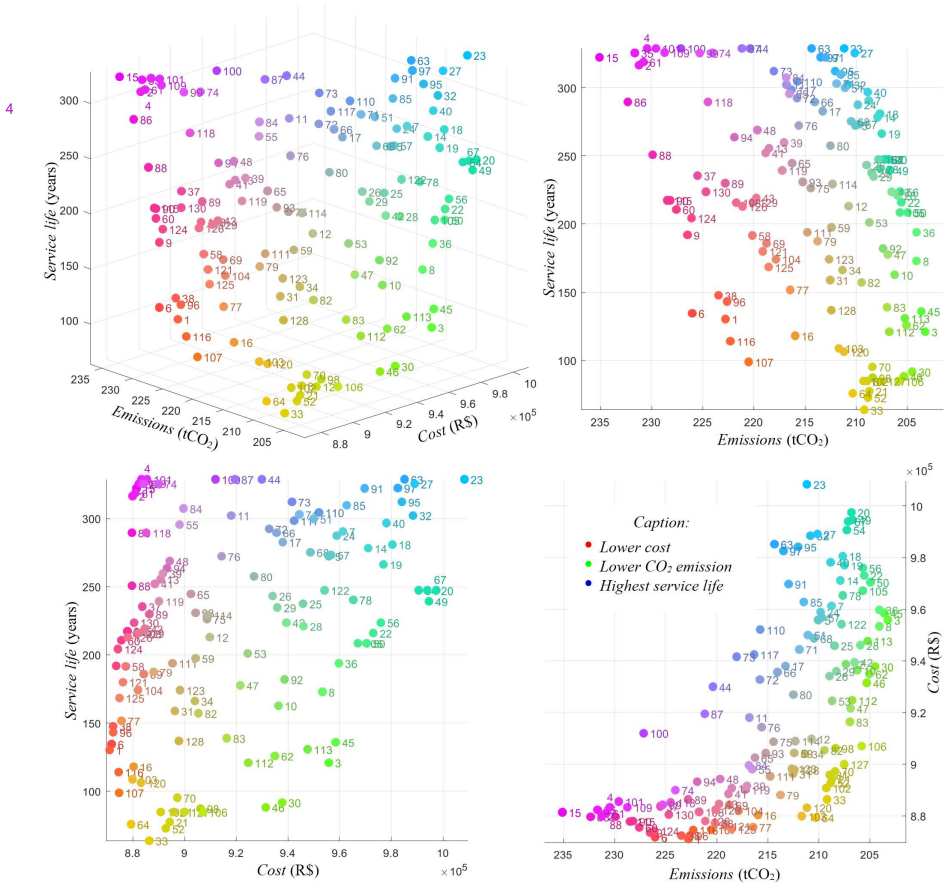

Figure 4. Objective function values of the optimal solutions – Atalaia

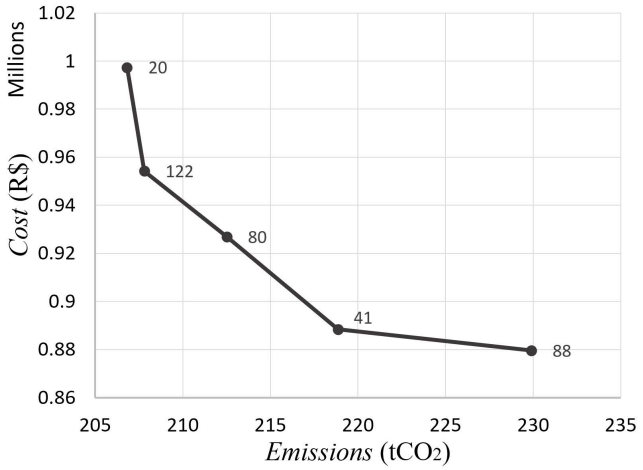

Figure 5. Cost - CO2 Emission relationship – Atalaia

The relationship between cost and service life of the solutions can vary according to the emissions range they belong to. To better understand this relationship, two samples of solutions were selected. The first sample included solutions 1, 9, 99, 124, and 130, with an average emission of 225 tCO_2. The second sample included solutions 27, 53, 68, 82, and 120, with an average emission of 210 tCO_2. These data are available in Figure 6.

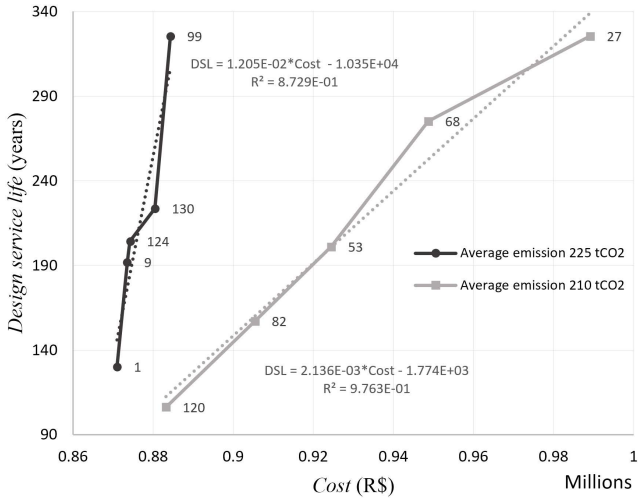

Figure 6. Cost - Design service life relationship – Atalaia

When analyzing these data through linear regression, it was observed that each additional decade of service life corresponds to a cost change for the solutions. In the first sample, an increase of one decade in service life correlates with a cost increase of R$ 829.88. In contrast, for the second sample, the cost increase per decade is substantially higher, at R$ 4,681.65.

Examining specific cases is useful to better understand the relationship between service life and cost. For instance, when comparing solution 1 with solution 99, a 150% increase in service life is associated with only a 1.5% increase in cost. In a different comparison, solution 120 versus solution 27 shows a 206% increase in service life, accompanied by a 12% increase in cost. These comparisons highlight the variable cost implications of extending service life in structural designs.

To assess the relationship between CO_2 emissions and service life, two sets of solutions were selected for analysis. The first set includes solutions 10, 17, 26, 30, and 73, with an average cost of R$ 0.88 million. The second set comprises solutions 2, 37, 64, 77, and 126, with an average cost of R$ 0.94 million. Details of these data are illustrated in Figure 7.

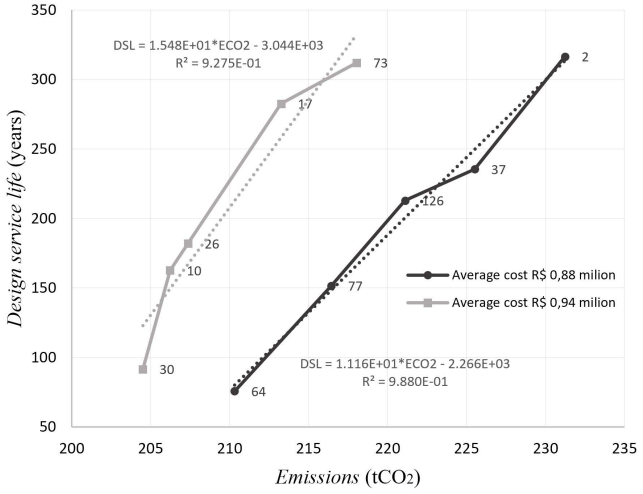

Figure 7. Emissions - Design service life relationship – Atalaia

By applying linear regression to these solutions, it was noted that the relationship between CO_2 emissions and service life correlates with the average cost of the solutions. Specifically, for solutions costing an average of R$ 0.88 million, there is a change of 0.896 tCO_2 per decade of service life. In contrast, solutions with an average cost of R$ 0.94 million show a change of 0.646 tCO_2 per decade of service life.

Comparing solution 64 with solution 2 reveals that a 76.1% increase in service life can be achieved with only a 9.0% increase in CO_2 emissions. Similarly, comparing solution 30 with solution 73 shows that service life can be increased by 70.7% with a corresponding 6.2% increase in emissions.

Figure 8 illustrates the degrees of freedom for the optimization solutions through a parallel coordinate plot. In this visualization, the degrees of freedom are displayed as parallel vertical axes, intersected by lines representing individual

solutions. The symbols denoting the DOF correspond to those defined in section 2.2. Additionally, the color coding of the lines follows the same scheme used in Figure 4, aiding in consistent interpretation across figures.

Using this representation for the DOF, along with the consistent color scheme, simplifies the process of identifying behavioral patterns within different regions of the solution space. The analysis of the parallel coordinates plot reveals that solutions with lower construction costs often achieve better fitness by opting for smaller concrete covers for columns and pier caps, combined with higher concrete strength. These solutions generally employ a contrasting approach for the deck, where a larger concrete cover is paired with lower concrete strength. Conversely, solutions with lower environmental impact reverse this arrangement. To optimize fitness, they incorporate larger concrete covers with lower concrete strength for columns and pier caps, while the deck utilizes higher concrete strength coupled with smaller concrete covers.

Another noteworthy observation is that degrees of freedom that increase the cross-sectional dimensions tend to yield solutions with lower costs, whereas those involving smaller cross-sectional dimensions typically lead to solutions with lower CO_2 emissions. The exception to this pattern is the width of the girder's upper flange, where larger values lead to lower CO_2 emissions and smaller values correspond to lower costs. A sensitivity analysis on this variable shows that reducing the width of the girder's upper flange extends the span of the slab, thereby increasing its cost. However, this increase in slab span impacts the overall cost less significantly in solutions with thicker slabs, which explains the divergent behavior observed with other degrees of freedom.

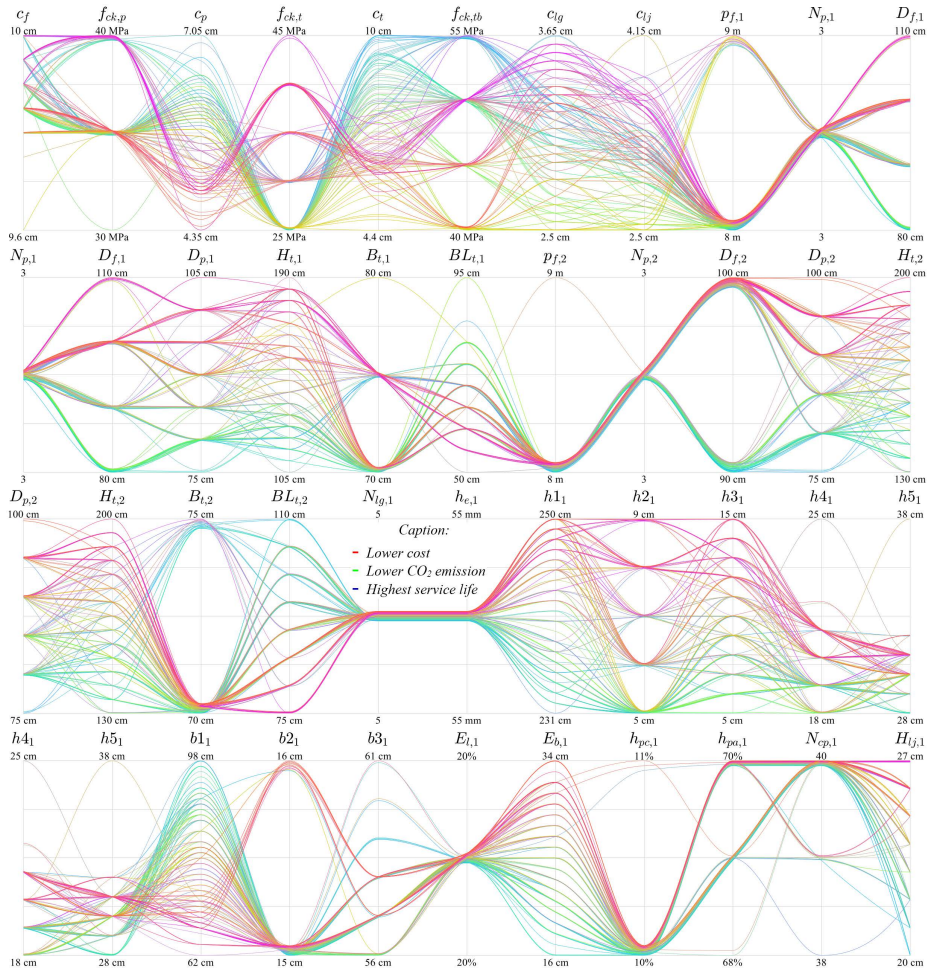

Figure 8. Parallel coordinates plot of the degrees of freedom – Atalaia

All solutions derived from the optimization process are non-dominated, indicating that improvements in one objective function invariably lead to compromises in another. This characteristic affords decision-makers the flexibility to select a solution that aligns best with their specific criteria. The authors recommend using the global cost per year of service as the selection criterion, denoted by $C_{g/t}$ and evaluated with Equation 8. This metric is computed by summing the construction costs and the costs associated with carbon credits, then dividing the total by the design service life of the project.

$$C_{g/t} = \frac{C_c + E_{tCO_2} \cdot C_{tCO_2}}{t_{DSL}} \quad (8)$$

where:

C_c: construction cost; E_{tCO_2}: environmental impact measured in tCO_2 emissions; C_{tCO_2}: cost of carbon credits, 153.53 R$/$tCO_2$ in the American market, according to [37]; and t_{DSL}: design service life in years.

The original project solution incurs a global cost per year of service amounting to 22,739.81 R$/year. All solutions within the optimal set demonstrate a reduction in this cost, showing improvements ranging from 36.5% to 87.7% compared to the original project proposal. Based on the criterion of selecting the solution with the lowest global cost per year of service, solution 4 is recommended, which offers a significantly reduced cost of 2,794.79 R$/year.

4.2. Case study of the viaduct in Mandaguaçu

The second case study, located in Mandaguaçu, features a 45.74 meters long viaduct divided into three spans, with a width of 12.4 meters and a road grade elevation as illustrated in Figure 9. The N_{spt} used in Figure 9 refers to the Standard Penetration Test *N*-value. Additional details necessary for defining the problem are provided in [24].

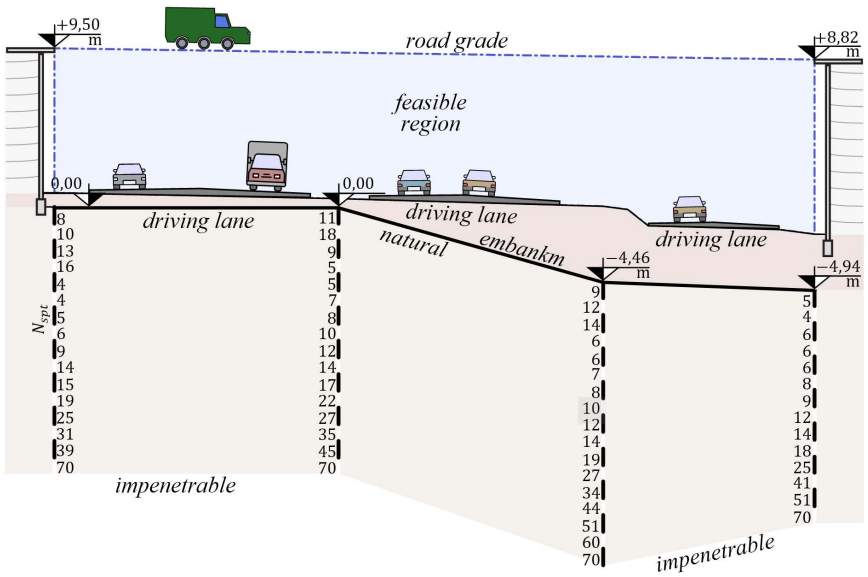

Figure 9. Optimization problem of the first case study – Mandaguaçu

The details of the constructed structure were obtained from the structural design provided by the original project's author. The design includes three spans measuring 17.10 m, 15.92 m, and 12.72 m, each supported by five girders with a height of 1.53 m. Each pier cap is supported by two columns; the first two supports have a diameter of 100 cm, while the last two supports are 120 cm in diameter. The shafts match the diameter of their corresponding columns and have a depth of 16 m, except for the fourth support, which is 14 m deep. Comprehensive details of the constructed solution are available in [24], and Figure 10 visually depicts this configuration.

For the original solution, the construction cost, CO_2 emissions, and design service life have been evaluated as outlined in section 2.1. The values for these objective functions, calculated based on the solution proposed by the project's author, are presented in Table 4.

The optimization for this case study was conducted using the UFSCar cluster and completed after 48 hours of analysis. The objective function values of the optimal solutions derived from this process are depicted in Figure 11.

Analysis of the solutions reveals that nearly the entire optimal set outperforms the original proposal across all objective functions. Exceptions include solutions 13, 38, 42, 45, and 70, which, despite offering lower cost and environmental impact, exhibit shorter service lives than the original solution. The optimal solutions demonstrate a reduction in construction cost ranging from 9.1% to 23.2%, a decrease in CO_2 emissions from 12.7% to 23.5%, and an increase in project service life by up to 540.7%.

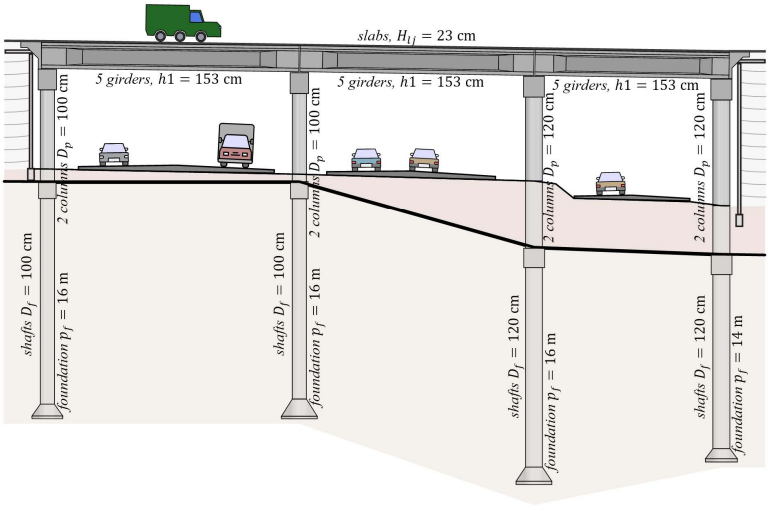

Figure 10. Original solution of the second case study – Mandaguaçu

Table 4. Objective functions for the original solution of the second case study – Mandaguaçu

Construction cost	Environmental impact	Design service life
R$ 1,556,206.74	372.90 tCO_2	51.3 years

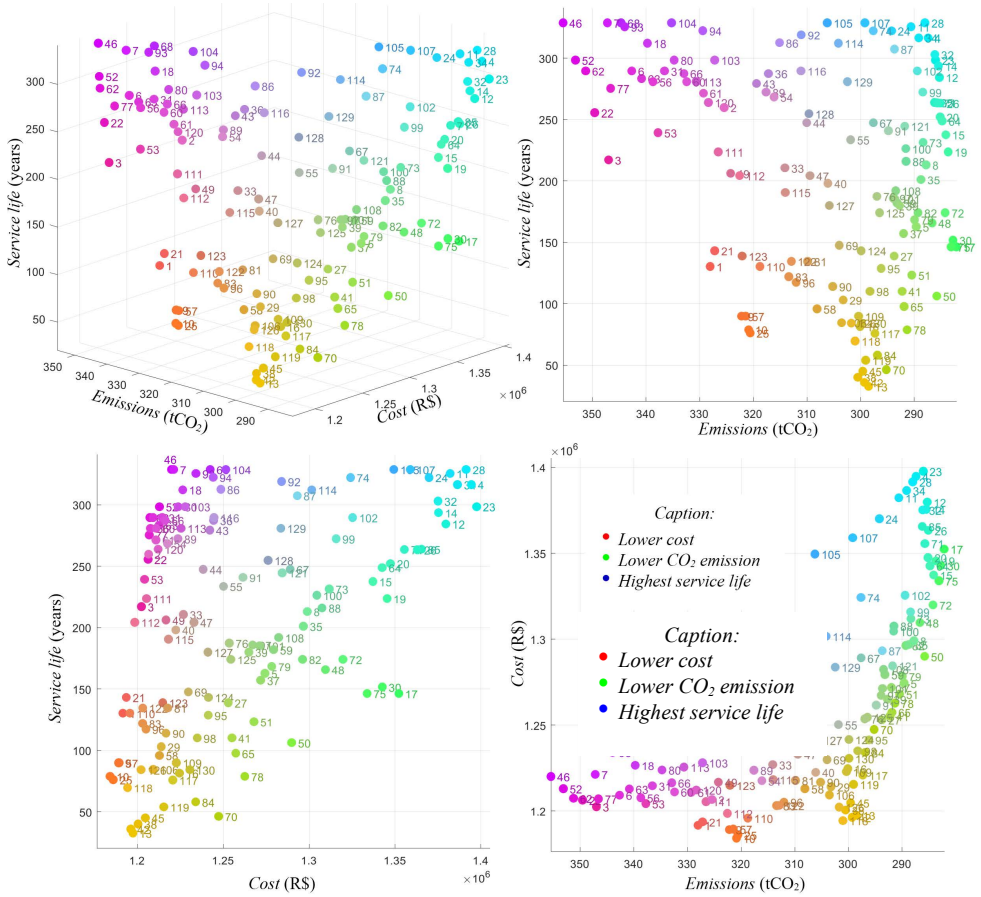

Figure 11. Objective function values of the optimal solutions – Mandaguaçu

By analyzing solutions 14, 62, 66, 102, and 116, which share similar service lives, a relationship between cost and CO_2 emissions becomes apparent, as shown in Figure 12. For instance, when comparing the objective functions of solution 62 to solution 66, it is possible to reduce environmental impact by 5.2% with only a minimal cost increase of 0.74%. However, this relationship is not linear; for example, comparing solution 14 to 102, the proportion is almost reversed, resulting in a cost reduction of 3.6% and a CO_2 emissions increase of only 1.4%. Although these solutions have an average design service life of 290 years, these cost-emission trade-offs remain consistent across other service life ranges.

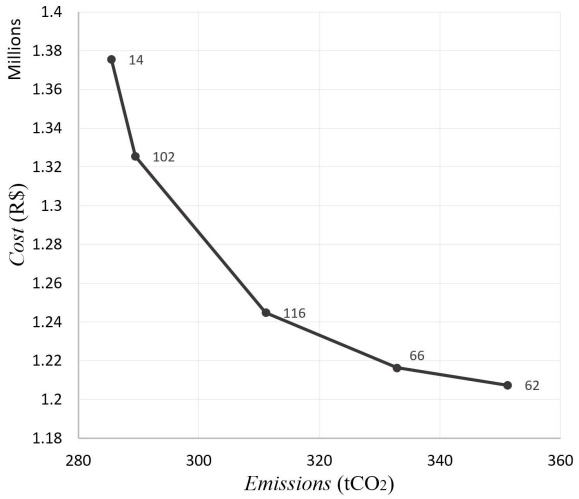

Figure 12. Cost - CO_2 Emission relationship – Mandaguaçu

The relationship between cost and service life of solutions can vary according to the emissions range to which they belong. To explore this relationship further, two groups of solutions were selected for analysis. The first group consists of solutions 10, 21, 103, 111, and 120, with an average emission of 326 tCO_2. The second group includes solutions 78, 82, 99, 100, and 102, with an average emission of 290 tCO_2. These data are illustrated in Figure 13.

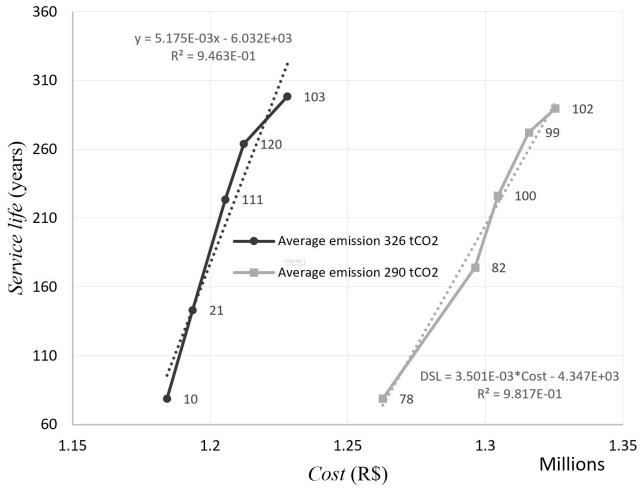

Figure 13. Cost - Design service life relationship – Mandaguaçu

Analysis of these data, fitted to linear equations, revealed that each decade of service life impacts the cost of solutions. For the first sample of solutions, every additional decade of service life correlates with a cost increase of R$ 1,932.37. In contrast, for the second sample, the increase per decade is more substantial, amounting to R$ 2,856.33.

Comparing specific solutions allows for establishing the relationship between service life and cost. For instance, the comparison between solution 10 and solution 103 shows that a 73.6% increase in service life results from a cost increase of only 3.6%. Similarly, the comparison between solution 78 and solution 102 indicates that a 72.8% extension in service life accompanies a 4.7% increase in cost.

To investigate the relationship between CO_2 emissions and design service life, two groups of solutions were selected based on their costs. The first group, consisting of solutions 49, 52, 81, 111, and 119, averages a cost of R$ 1.21 million. The second group, including solutions 50, 82, 87, and 121, has an average cost of R$ 1.29 million. These data are presented in Figure 14.

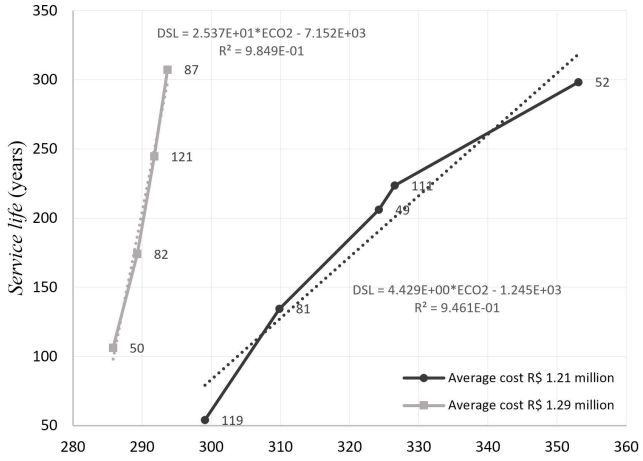

Figure 14. Emissions - Design service life relationship – Mandaguaçu

Upon fitting these solutions to linear equations, it was noted that the relationship between CO_2 emissions and service life correlates with the average cost of the solutions. Specifically, solutions with an average cost of R$1.21 million are associated with a change of 2.258 tCO_2 per decade of service life, whereas those costing R$1.29 million experience a smaller change, amounting to 0.394 tCO_2 per decade.

To highlight the differences in trade-offs between objective functions, a comparison between solution 119 and solution 52 shows an 81.9% increase in service life, accompanied by a 15.3% rise in CO_2 emissions. In contrast, comparing solution 50 with solution 87 demonstrates a service life increase of 65.4%, but with a smaller increase in emissions of only 2.7%. These comparisons illustrate the variability in the relationship between service life extension and CO_2 emissions across different regions of the solution space.

The parallel coordinates plot, shown in Figure 15, depicts the degrees of freedom for the optimization solutions. This visualization, along with the utilized color scheme, aids in identifying behavioral patterns across various regions of the solution space.

Analysis of the parallel coordinates plot reveals that the pattern observed in the Atalaia case study, which leads to the highest service life values, is also evident in the Mandaguaçu case study. Additionally, it is consistently observed that degrees of freedom increasing the cross-sectional areas tend to yield solutions with lower costs, whereas smaller cross-sectional dimensions are associated with lower CO_2 emissions. The exception concerning the width of the top flange of the girder, as noted in the earlier result, persists in these results as well.

The original design solution incurs a global cost per year of service amounting to 31,451.42 R$/year. All solutions in the optimal set, except for those with a shorter service life than the original design, demonstrate a reduction in this cost, with improvements ranging from 29.8% to 87.7% compared to the original design. Based on the criterion of selecting the solution with the lowest global cost per year of service, solution 46 is recommended, as it presents a significantly reduced cost of 3,877.38 R$/year.

Figure 15. Parallel coordinates plot of the degrees of freedom – Mandaguaçu

5. CONCLUSIONS

This paper presents the MOPSO method, with parameters calibrated by [15], to optimize viaducts, assessing two real case studies. Both case studies yielded similar results, demonstrating that the optimized solutions significantly outperformed the original designs across all evaluated objective functions.

For the Atalaia viaduct, the optimization process resulted in:

- reduction of construction costs by 10.5% to 22.7%;
- decrease in CO_2 emissions by 8.9% to 21.2%;
- extension of the design service life by 24.0% to 540.7%.

Similarly, the Mandaguaçu viaduct showed:

- cost reductions ranging from 9.1% to 23.2%;
- decrease in CO_2 emissions from 12.7% to 23.5%;
- increase in design service life by up to 540.7%.

The relationship between cost and CO_2 emissions in both Atalaia and Mandaguaçu case studies is non-linear, showing that this relationship is relatively the same regardless of the service life. In Atalaia, reducing environmental impact by 4.8% required only a 1.0% increase in cost, whereas in Mandaguaçu, a 5.2% emissions reduction was achieved with a minimal 0.74% cost increase. These findings illustrate that cuts in emissions can be achieved with modest increases in costs, aligning with the findings of [11].

The design service life represented the objective function with the greatest performance gain compared to the original project design. These gains are due to the initially low service life of the original design and, although substantial, should be considered purely theoretical. This is because the top-performing solutions indicate a durability that exceeds 300 years, an estimate that surpasses the practical usage expectations of most structures. Similar to reference [11], we did not limit the value of service life in our analyses, allowing for a broader comparison of potential improvements. Moreover, the relationships between cost and service life, as well as CO_2 emissions and service life, appear to be linear. Importantly, the addition of cost per year of service proves to be justified, because, in both cases, the solutions that offered the best global cost per year of service were those that exhibited the longest service life. By implementing an upper limit for the design service life, the performance of the optimal solutions in terms of global cost per year of service would be reduced. However, even with this limitation, these values would still be higher than those of the original design.

Analysis of the degrees of freedom in relation to the objective functions in the Atalaia and Mandaguaçu case studies revealed clear patterns. For instance, solutions that minimized construction costs tended to opt for smaller concrete covers combined with higher concrete strength for columns and pier caps, while the deck construction utilized larger concrete covers paired with lower concrete strength. Conversely, solutions aiming to lower environmental impact adopted the opposite approach, highlighting the strategic manipulation of concrete cover and strength to achieve specific cost or environmental objectives. Additionally, it was observed that increasing the cross-sectional dimensions generally led to cost reductions, while smaller dimensions favored lower CO_2 emissions.

The analysis of the global cost per year of service clearly demonstrates the advantage of optimized solutions over the original designs in both the Atalaia and Mandaguaçu case studies. The optimized solutions not only showed a significant reduction in the global cost per year of service compared to the original designs but also aligned these economic benefits with enhanced environmental performance. This finding supports the effectiveness of the optimization methodology in improving the sustainability and cost-efficiency of infrastructure projects, offering a compelling argument for its broader application.

REFERENCES

[1] K. Hashimoto, "Técnicas de otimização combinatória multiobjetivo aplicadas na estimação do desempenho elétrico de redes de distribuição," Ph.D. dissertation, Univ. de São Paulo, São Paulo, SP, Brazil, 2004. [Online]. Available: https://teses.usp.br/teses/disponiveis/3/3143/tde-19112004-165342/pt-br.php

[2] M. A. Hassanain and R. E. Loov, "Cost optimization of concrete bridge infrastructure," *Can. J. Civ. Eng.*, vol. 30, pp. 841–849, 2003, http://dx.doi.org/10.15554/pcij.07011993.60.78.

[3] E. V. W. Trentini "Otimização de seções de viadutos e pontes de múltiplas longarinas pré-moldadas e protendidas," M.S. thesis, Univ. Est. Maringá, Maringá, PR, Brazil, 2016. [Online]. Available: http://repositorio.uem.br:8080/jspui/handle/1/5691

[4] G. G. B. Torres, J. F. Brotchie, and C. A. Cornell, "A program for the optimum design of prestressed concrete highway bridges," *PCI J.*, vol. 11, no. 3, pp. 63–71, 1965, http://dx.doi.org/10.15554/pcij.06011966.63.71.

[5] Z. Lounis and M. Z. Cohn, "Optimization of precast prestressed concrete bridge girder systems," *PCI J.*, vol. 38, no. 4, pp. 60–78, 1993, http://dx.doi.org//10.15554/pcij.07011993.60.78.

[6] B. P. Olivieri, "Otimização do projeto de pontes protendidas pré-moldadas pelo método dos algoritmos genéticos," M.S. thesis, Inst. Alberto Luiz Coimbra de Pós-Grad. e Pesq. Eng., Univ. Fed. do Rio de Janeiro, Rio de Janeiro, RJ, Brazil, 2004. [Online]. Available: http://www.dominiopublico.gov.br/pesquisa/DetalheObraForm.do?select_action=&co_obra=133098

[7] C. F. M. Cortês, "Otimização do projeto da superestrutura de pontes pré-fabricadas pelo método dos algoritmos genéticos," Ph.D. dissertation, Inst. Alberto Luiz Coimbra de Pós-Grad. e Pesq. Eng., Univ. Fed. do Rio de Janeiro, Rio de Janeiro, RJ, Brazil, 2010. [Online]. Available: http://www.dominiopublico.gov.br/pesquisa/DetalheObraForm.do?select_action=&co_obra=181676

[8] R. Ahsan, S. Rana, and S. N. Ghani, "Cost optimum design of posttensioned I-girder bridge using global optimization algorithm," *J. Struct. Eng.*, vol. 138, no. 2, pp. 273–284, 2012, http://dx.doi.org/10.1061/(ASCE)ST.1943-541X.0000458.

[9] S. El Mourabit, "Optimization of Concrete Beam Bridges: Development of Software for Design Automation and Cost Optimization," M.S. thesis, KTH Royal Inst. Tech., Stockholm, Sweden, 2016. [Online]. Available: https://www.diva-portal.org/smash/get/diva2:945092/FULLTEXT01.pdf

[10] V. Yepes, T. García-Segura, and J. M. Moreno-Jiménez, "A cognitive approach for the multi-objective optimization of RC structural problems," *Arch. Civ. Mech. Eng.*, vol. 15, no. 4, pp. 1024–1036, 2015, http://dx.doi.org/10.1016/j.acme.2015.05.001.

[11] T. García-Segura, V. Yepes, and D. M. Frangopol, "Multi-objective design of post-tensioned concrete road bridges using artificial neural networks," *Struct. Multidiscipl. Optim.*, vol. 56, no. 1, pp. 139–150, 2017, http://dx.doi.org/10.1007/s00158-017-1653-0.

[12] C. Blum, "Metaheuristics in combinatorial optimization: overview and conceptual comparison," *ACM Comput. Surv.*, vol. 35, no. 3, pp. 268–308, 2003, http://dx.doi.org/10.1145/937503.937505.

[13] G. R. Zavala et al., "A survey of multi-objective metaheuristics applied to structural optimization," *Struct. Multidiscipl. Optim.*, vol. 49, no. 4, pp. 537–558, 2014, http://dx.doi.org/10.1007/s00158-013-0996-4.

[14] D. H. Wolpert and W. G. Macready, "No free lunch theorems for optimization," *IEEE Trans. Evol. Comput.*, vol. 1, no. 1, pp. 67–82, 1997, http://dx.doi.org/10.1109/4235.585893.

[15] E. V. W. Trentini, G. A. Parsekian, and T. N. Bittencourt, "Multiobjective optimization of bridge and viaduct design: Comparative study of metaheuristics and parameter calibration," *Eng. Struct.*, vol. 312, pp. 118252, 2024, https://dx.doi.org/10.1016/j.engstruct.2024.118252.

[16] Departamento Nacional de Infraestrutura de Transportes, "Sistema de Custos Referenciais de Obras - SICRO, Relatório Sintético de Composições de Custos, São Paulo - Abril/2022," Brasília: Coord. Geral de Custos de Infraestrutura de Transportes, 2022. [Online]. Available: https://www.gov.br/dnit/pt-br/assuntos/planejamento-e-pesquisa/custos-e-pagamentos/custos-e-pagamentos-dnit/sistemas-de-custos/sicro_antiga/sudeste/espirito-santo/2022/abril/abril-2022 (accessed Apr. 26, 2023).

[17] B. L. C. Costa, "Quantificação das emissões de CO2 geradas na produção de materiais utilizados na construção civil no Brasil," M.S. thesis, Inst. Alberto Luiz Coimbra de Pós-Grad. e Pesq. Eng., Univ. Fed. do Rio de Janeiro, Rio de Janeiro, RJ, Brazil, 2012. http://dx.doi.org/10.13140/RG.2.1.2161.8801.

[18] E. Possan, J. J. O. Andrade, and D. C. C. Dal Molin "Model to Estimate Concrete Carbonation Depth and Service Life Prediction," in *Hygrothermal Behaviour and Building Pathologies*, J. M. P. Q. Delgado, Ed., Cham: Springer, 2021, pp. 67-97, https://doi.org/10.1007/978-3-030-50998-9_4.

[19] Associação Brasileira de Normas Técnicas, "*Projeto de pontes de concreto armado e de concreto protendido – Procedimento,* ABNT NBR 7187:2021, 2021.

[20] Associação Brasileira de Normas Técnicas, *Projeto de Estruturas de Concreto* – Procedimento, ABNT NBR 6118:2014, 2014.

[21] Associação Brasileira de Normas Técnicas, *Carga móvel rodoviária e de pedestres em pontes, viadutos, passarelas e outras estruturas – Procedimento*, ABNT NBR 7188:2013, 2013.

[22] E. Winkler, *Die Lehre von der Elastizität und Festigkeit mit besonderer Rücksicht auf ihre Anwendung in der Technik für Polytechnische Schulen, Bauakademien, Ingenieure, Maschinenbauer, Architecten, etc*. Prague, Czech Republic: Dominicius, 1868.

[23] G. C. G. Barros and L. F. Martha, "Consideração de barras rígidas e inextensíveis na análise matricial através da programação matemática," *Rev. Interdiscip. Pesq. Eng.*, vol. 2, no. 27, pp. 1-16, 2016, https://doi.org/10.26512/ripe.v2i27.14451.

[24] E. V. W. Trentini, "Otimização de projeto de viadutos de múltiplas longarinas considerando critérios ambientais e econômicos," Ph.D. dissertation, Univ. Federal de São Carlos, São Carlos, SP, Brazil, 2023. [Online]. Available: https://repositorio.ufscar.br/handle/ufscar/18157

[25] M. K. El Debs and T. Takeya, *Introdução às pontes de concreto*. São Paulo, SP, Brazil: Universidade de São Paulo, 2010.

[26] M. K. El Debs, *Pontes de concreto: com ênfase na aplicação de elementos pré-moldados*, 1st ed., São Paulo, SP, Brazil: Oficina de Textos, 2021.

[27] PRECAST/Prestressed Concrete Institute, *PCI Design Handbook: Precast and Prestressed Concrete*, 7th ed., Chicago: PCI, 2010.

[28] P. A. Krahl, M. C. V. Lima, and G. H. Siqueira, "Simplified analytical nonlinear model for contact problem between precast concrete beams and elastomeric bearing pads," *J. Struct. Eng.*, vol. 146, no. 11, pp. 04020251, 2020, http://dx.doi.org/10.1061/(ASCE)ST.1943-541X.0002822.

[29] Associação Brasileira de Normas Técnicas, *Projeto e execução de estruturas de concreto pré-moldado*, ABNT NBR 9062:2017, 2017.

[30] E. V. W. Trentini, G. A. Parsekian, and T. N. Bittencourt, "A method for considering the influence of distinct casting stages in the flexural design of prestressed concrete cross sections," *IBRACON Struct. Mater. J.*, vol. 15, no. 4, pp. e15410, 2022, http://dx.doi.org/10.1590/S1983-41952022000400010.

[31] P. S. S. Bastos, *Blocos de Fundação*. Universidade Estadual Paulista, 2020. [Online]. Available: https://wwwp.feb.unesp.br/pbastos/concreto3/Blocos.pdf (accessed Apr. 26, 2023).

[32] W. Hachich et al., *Fundações – Teoria e prática*, 2. ed., São Paulo, SP, Brazil: Pini, ABMS/ABEF, 1998.

[33] J. C. A. Cintra, N. Aoki, and J. H. Albiero *Fundações Diretas: Projeto Geotécnico*, São Paulo, SP, Brazil: Oficina de Textos, 2011.

[34] J. Kennedy and R. C. Eberhart *Swarm Intelligence*, Burlington, MA, USA: Morgan Kaufmann Publishers, 2001, https://doi.org/10.1007/0-387-27705-6_6.

[35] C. A. C. Coello, G. T. Pulido, and M. S. Lechuga, "Handling multiple objectives with particle swarm optimization," *IEEE Trans. Evol. Comput.*, vol. 8, no. 3, pp. 256–279, 2004, http://dx.doi.org/10.1109/TEVC.2004.826067.

[36] C. R. Raquel and C. N. J. Prospero, "An effective use of crowding distance in multiobjective particle swarm optimization," in *Proc. 7th Annual Conf. on Genetic and Evolutionary Computation (GECCO '05)*, New York, NY, USA: Association for Computing Machinery, Jun. 2005, pp. 257-264, http://dx.doi.org/10.1145/1068009.1068047.

[37] Carbon Credits Inc. "Live Carbon Prices Today," CarbonCredits.com. Available: https://carboncredits.com/carbon-prices-today (accessed Apr. 26, 2023).

Author contributions: EVWT: conceptualization, development of the computational algorithm, data analysis, writing and translation; GAP and TNB: supervision, revision, translation.

Editors: Diogo Ribeiro, Daniel Cardoso.